A STUDY ON WEAR LOCATIONS FOR HP TURBINE EXTRACTION PIPING IN THE MAANSHAN NUCLEAR POWER PLANT

N. M. Chung, L. C. Wang
Taiwan Power Company, Taiwan, China

Y. P. Ma, Y. M. Ferng
Institute of Nuclear Energy Research, Taiwan, China

ABSTRACT

Due to the high velocity, relatively low quality and chemical properties of steam, the erosion/corrosion wear are significant in the piping of the BOP (balance of plant) system. A break of the extraction line of the high pressure turbine (HPTB) had occurred in unit #2 of the Maanshan Nuclear Power Plant (NPP). Therefore, the potential wear locations are investigated by the aids of computational fluid dynamics (CFD). In the model, the impingement of liquid droplets on the wall is assumed to be the dominating mechanism to remove wall material. Thus, three-dimensional two-phase flow field is calculated and a wear model is also developed to help determine the potential wear locations. The inlet geometry is modeled to study the upstream effect and the downstream piping layout is also considered. The calculated data are compared to the inspection ones that are reproduced from inspections of pipe wall thickness measured by ultrasonic transmitters (UT) in the Maanshan NPP. The results show the present approach is reasonable and may be a potential tool to identify the regions with higher wear rates.

INTRODUCTION

Erosion/corrosion is an old problem in piping systems. Basically, it involves two mechanisms, one is mechanical erosion and the other is chemical corrosion. The pipe wall is worn under the combined actions of these two mechanisms and the wall thickness is dramatically reduced after several-years' operation. Erosion/corrosion problem did not attract too much attention until the time when the feed water line break accident occurred in the Surry Nuclear Power Plant in 1986. After the accident, the Nuclear Regulation Commission started to request NPPs to provide a long-term wall thickness monitoring program for safety. Taiwan Power Company started the monitoring program with the help of the CHEC series computer code, which was developed by the Electrical Power Research Institute (EPRI), from 1994 . However, the program increases the staff's loading a lot during the outage of NPP. Recently, an extract line break occurred due to erosion/corrosion in the Maanshan NPP and resulted in a shutdown lasting several days. If the break location could have been predicted and notified in advance, the incident might be avoided. In the past years, we have struggled for developing an effective method that can identify the most probable local erosion/corrosion regions. This paper thus reports the approaches and the results of the analysis on the wear locations of HPTB extraction piping in the Maanshan NPP. So far, most of the studies on erosion/corrosion or the predictions of wear rate are based on macroscopic viewpoint(Keck & Griffith, 1987, Chexal et. al. 1993). The approaches are based on correlation and empirical constants. So that they can 't predict the most dangerous locations of piping and the effects of piping layout, which is related to local flow information. Physically, the factors of erosion/corrosion include piping material, pH, fluid temperature, dissolved oxygen, fluid velocity, quality and piping geometry etc. .Nesic and Postlethwaite (1991) studied the localized erosion/corrosion wear rate by the combinations of the flow, the corrosion and the erosion models. However, due to too much uncertainty, efforts are still needed to improve the accuracy. In our study, local flow field and fluid properties of the piping are thought to be the dominant factors that control the wear locations. So three dimensional fluid flow structures are necessary and the CFD code CFX-4.1 (1994) is used for convenience. To benchmark the model. the calculated data are also compared to the inspection ones measured by UT. Moreover the effects of upstream and downstream piping are also studied. The calculated data show good agreement with the inspection data and it seems encouraging that the approach may identify the local dangerous regions of piping.

MECHANISMS, MODEL AND ANALYSIS

There are two interacting mechanisms occurring in erosion/corrosion: one is mechanical erosion and the other chemical corrosion. The wear will be dramatically reduced without either one of the two mechanisms. Based on the experiences and observations, wear is seldom found in piping made of alloy or operated at quality higher than 99% (Ma et. al., 1996) since no corrosion occurs, for example. Generally speaking, oxide will be formed as long as water flows over the steel surface and the corrosion rate will be dependent on chemical reaction. As for erosive mechanisms, there are two: one is dissolution wear and the other is droplet impact wear (Keck & Griffith, 1987) . The oxide formed on the steel in a stagnant fluid will finally be equilibrium and the reaction stops. However, if the flow is moving, the concentration gradient will be established near the wall and the oxide is continuously dissolved and removed by convection, which results in wall thinning. On the other hand, the droplet impact wear is caused by direct impacts from liquid drops that are entrained in the bulk vapor flow. Droplet flow pattern always occurs at two-phase flow piping with higher quality. The liquid drop impinges on the oxidized wall surface repeatedly and the oxide is finally removed. In the present study, the droplet impact wear mechanism is assumed to be more dominant than the other one because the analyzed piping system is operated at a quality of 92% and the flow pattern is assumed to be droplet flow.

Maanshan NPP, which is a Pressurized Water Reactor (PWR), has a set of high and low pressure turbine in the secondary side. Some of the steam in the HP turbine is extracted to preheat the feed water by an extraction piping system. The damaged extraction pipe line, on which the present study focuses, is the third-stage extraction which serves the first-stage heater. After the steam passing the third-stage moving blades, some of the steam is extracted into a cavity through a tiny circumferential slot. Then the steam flows into the extraction line, which connects to the cavity on the bottom of the turbine body, through the circumferential cavity passage. Because the design quality of the extraction piping system is relatively low (92%), the flow must be two-phase. The droplets and perhaps liquid film which may form along the cavity wall, flow down into the extraction piping along with steam flow. Under the present assumptions, the droplets continuously and repeatedly impinge on somewhere of the pipe wall. The locations of impingement depend on the flow structures and the geometry of flow passages. The schematic of the HPTB extract pipe line is shown as Figure 1. To obtain the most probable wear locations the geometry of flow passages have to be modeled carefully. In the present analysis, the flow passages of the circumferential slot and cavity are assumed to be a quarter model, as shown in Figure 2, to save computational efforts but not to deteriorate the real physical behaviors, especially for upstream geometry of the piping. Total mass flow rate is assumed flowing uniformly through the circumferential slot, so that three quarters of the total flow rate is assumed to flow equally into both inlets of the cavity passage. The inlet boundary conditions are thus determined by two-phase homogeneous model with a designed total mass flow rate of 46.8 kg/s and 92% quality. The diameter of the piping is 12 inches, and the operating pressure and temperature are 2.776 MPa and 229.2C respectively. To include the effects of downstream piping layout two horizontal elbows (No.2036 and 2037) just succeeding the vertical extraction line are also modeled. The outlet boundary condition is set to be mass conservation, i.e. the mass flow rate of outlet and inlet is the same.

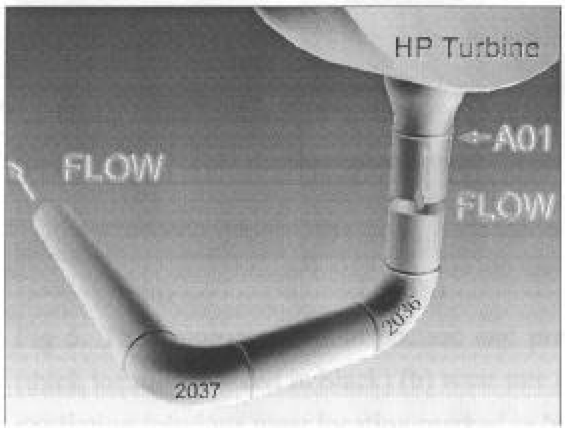

Fig. 1 Schematic of HPTB extraction line

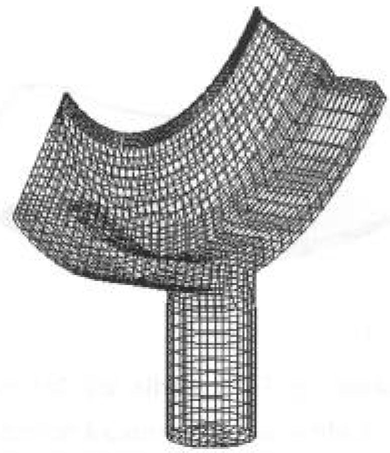

Fig. 2 Mesh grid of HPTB extraction line

Since the local flow structures are necessary in the analysis, the commercial CFD code, CFX-4.1, is used for this purpose. CFX-4.1 uses finite volume method on a non-orthogonal body-fitted grid and has a user-friendly interface structure where options can be selected by the user. The options includes models, solution schemes and I/O controls etc. The flow pattern is assumed to be two-phase droplet flow and the drops are entrained by the bulk vapor flow in the analysis, two phases, i.e. steam phase and liquid phase are governed by each phase's Navier-Stoke equation, which is called multifluid model. The coupling between phases is through mass, momentum and energy transfers. However mass and energy coupling are neglected in this case. The convergence criteria is set to be that the mass residual is less than 10^{-3} relative to inlet mass flow rate. Other assumptions of the analysis are:

(1) Drag force between phases is considered in the momentum equation, and drag coefficient was assumed to be a constant, 0.44.

(2) Droplet diameter is constant and assumed to be spherical.

(3) Pressure is the same for phases.

Standard k-ε model is selected in the turbulent model and wall function is used for each phase.

The governing equations calculated in the code are,

The Continuity equation:

$$\frac{\partial}{\partial t}\left(r_\alpha \rho_\alpha\right) + \nabla \bullet \left(r_\alpha \rho_\alpha \vec{U}_\alpha\right) = 0 \qquad \text{..................................} \quad (1)$$

Where r is the void fraction, ρ is the density, $\vec{U}$ is the velocity vector and the subscript α represents a liquid or gas phase.

The Momentum equation:

$$\frac{\partial}{\partial t}\left(r_\alpha \rho_\alpha \overrightarrow{U_\alpha}\right) + \nabla \bullet \left(r_\alpha \left(\rho_\alpha \overrightarrow{U_\alpha} \otimes \overrightarrow{U_\alpha} - \mu_{\alpha \mathrm{eff}} \left(\nabla \overrightarrow{U_\alpha} + \left(\nabla \overrightarrow{U_\alpha} \right)^{T} \right)\right)\right)$$

$$= r_\alpha \left(\vec{B} - \nabla P \right) + \sum_\beta C_{\alpha\beta}^{(d)} \left(\overrightarrow{U_\beta} - \overrightarrow{U_\alpha} \right) \tag{2}$$

Where P is pressure, $\vec{B}$ is gravity vector and $\mu_{\alpha \mathrm{eff}}$ is effective viscosity

$$\mu_{\alpha \mathrm{eff}} = \mu + \mu_{T\alpha} \tag{3}$$

Turbulent kinetic energy:

$$\frac{\partial}{\partial t}\left(r_\alpha \rho_\alpha k_\alpha\right) + \nabla \bullet \left(r_\alpha \left(\rho_\alpha \overrightarrow{U_\alpha} k_\alpha - \left(\mu + \frac{\mu_{T\alpha}}{\sigma_k} \right) \nabla k_\alpha \right)\right) = r_\alpha \left(P_\alpha - \rho_\alpha \varepsilon_\alpha \right) \tag{4}$$

With:

$$\mu_{T\alpha} = C_\mu \rho_\alpha \frac{k_\alpha^2}{\varepsilon_\mu} \tag{5}$$

$$P_\alpha = \mu_{\alpha \mathrm{eff}} \nabla \vec{U}_\alpha \bullet \left[\nabla \vec{U}_\alpha + \left(\nabla \vec{U}_\alpha \right)^{T} \right] - \frac{2}{3} \nabla \bullet \vec{U}_\alpha \left(\mu_{\alpha \mathrm{eff}} \nabla \bullet \vec{U}_\alpha + \rho k_\alpha \right) \tag{6}$$

Where k_α is turbulent kinetic energy for phase α , σ_k is turbulent Prandtl number and $\mu_{T\alpha}$ is eddy viscosity for phase α

The turbulent energy dissipation equation:

$$\frac{\partial}{\partial t}\left(r_\alpha \rho_\alpha \varepsilon_\alpha\right) + \nabla \bullet \left(r_\alpha \left(\rho_\alpha \overrightarrow{U_\alpha} \varepsilon_\alpha - \left(\mu + \frac{\mu_{T\alpha}}{\sigma_\varepsilon} \right) \nabla \varepsilon_\alpha \right)\right) = r_\alpha \frac{\varepsilon_\alpha}{k_\alpha} \left(C_{1\varepsilon} P_\alpha - C_{2\varepsilon} \rho_\alpha \varepsilon_\alpha \right) \tag{7}$$

Where ε_α is turbulent dissipation rate for phase α .The empirical constants are set to the standard for k-ε equation, i.e. C_μ =0.09, σ_ε =1.3, $C_{1\varepsilon}$ =1.44 and $C_{2\varepsilon}$ =1.92.

The time derivatives in the governing equations can be omitted since steady state is assumed in the present analysis. To solve the governing equations numerically the computational domain has to be discretized. CFX4.1 provide a powerful pre-processor to serve this purpose. Body-fitted coordinate and multi-block methods are used to establish the computational grid system with 25 blocks and about 9,000 grids. The typical grid system of the inlet part of extraction piping is shown as Figure 2. Moreover, about a 45,000 grid system is also established to test the convergence of the flow. To validate the effects of upstream and downstream piping components, and the effect of droplet diameter, several combinations of sensitivity study are also tested .Since the impact wear is assumed to be the dominant mechanism for the wall to be worn, the removed mass is generally represented by (1988)

$$\dot{m} = CF(\theta) \frac{\rho u^2}{H} \tag{8}$$

Where C is constant, F is the impact angle function, H is hardness and u is impact velocity. If the total kinetic energy of liquid drops colliding the wall is transferred to the energy to remove the corrosion layer. So the wear indicator can be defined for the present purpose to predict wear location as follows:

$$I = a_f \times u_n \times |u_n| \tag{9}$$

Where u_n is velocity normal to the wall and a_f is liquid volume fraction. Since the flow is assumed to be non-slip on the wall, the velocity of the grids just next to the wall is selected to calculate u_n .This approach may result in inconsistent results for sharply changing geometry, but it is not serious for the piping with same size. It is worth to note that the absolute value of wear index, I, is meaningless, but the relative value of different locations may show the potential for the wear of the wall.

THE INCIDENT AND INSPECTION DATA

A bursting break, which is located about six inches below the welding ring between the third-stage extraction pipe line (AF-298-12", N1P) of HP turbine and turbine body, was found during normal operation in the early morning on June 14th 1996, just few weeks after the outage of EOC-9, at #2 of Maanshan NPP. Actually the pipe was covered in the inspection program during the outage. The most important reason for the thinning site not detected in time attributed to human error. Because the starting position (noted by A01 in Figure 1) to inspect was wrongly notified twelve inches below the welding ring of the piping and the most dangerous site was missed. Anyway, if some potential and probable thinning locations of the pipe could be notified in advance, the break incident may be avoided.

To validate the present approach, three sets of pipe wall thickness inspection data which include a straight pipe (N1P) and two succeeding elbows (E2036 and E2037), of the HPTB extraction line system of #1, are selected. The wall thickness data of the components are represented as gray level and the cylindrical piping surface is stretched into rectangular grid for demonstration. Azimuthal direction is noted on the figures from A to N in clockwise according to flow direction . Axial direction is noted by the number starting from 1 and the axial length of inspection is about two times of piping diameter. So the axial grid size is about three inches. Figures 3(a), 4(a) and 5(a) show the original wall thickness inspection data for N1P, E2036 and E2037. Inevitably, the inspection errors may exist and cause some sharp transition of thickness between two neighboring grids. To smear out the unreasonable phenomena the original thickness data are managed by averaging the eight neighboring data for each grid. At the same time the wear rate is calculated by the difference between the thickest data and grid data, and the operating time. The wear rates for N1P, E2036 and E2037 are also demonstrated by gray level and the same rectangular grid surface, as shown in Figures 3(b), 4(b) and 5(b). It is worth to note that locations with higher wear rate are marked in a blacker color in the part (b) of the figures, while it is locations with thicker wall in the part(a).

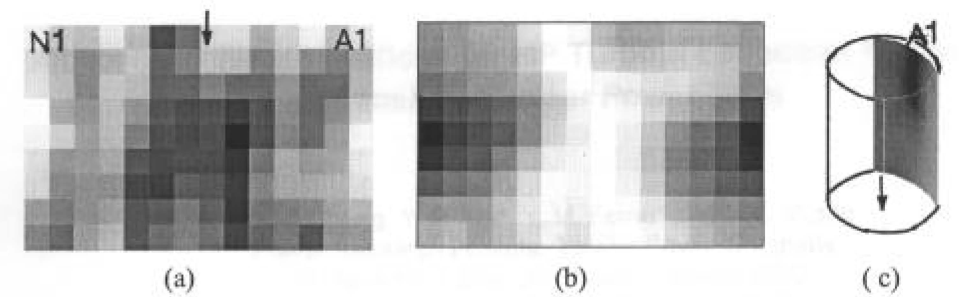

Fig 3. The comparison of inspection and prediction data for N1P straight pipe (a) thickness (thick location marked in black) (b) wear rate (severe wear location marked in black) (c) prediction (obvious wear location marked in black)

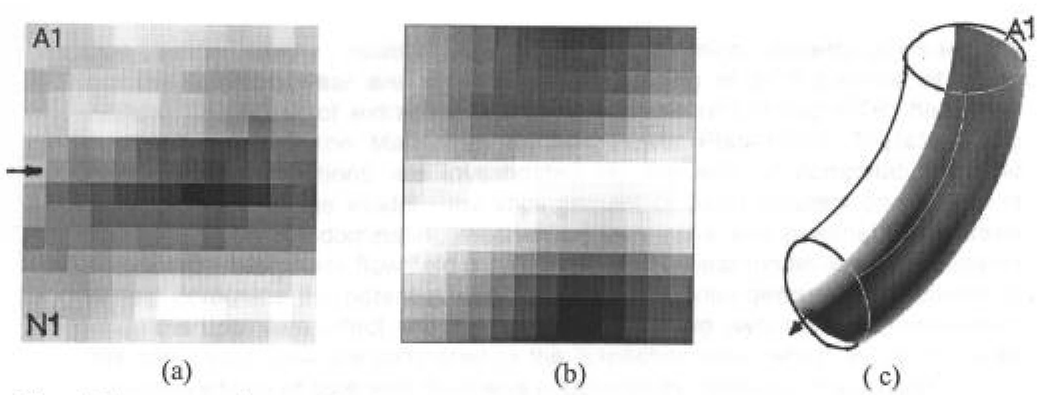

Fig 4. The comparison of inspection and prediction data for elbow 2036 (a) thickness (thick location marked in black) (b) wear rate (severe wear location marked in black) (c) prediction (obvious wear location marked in black)

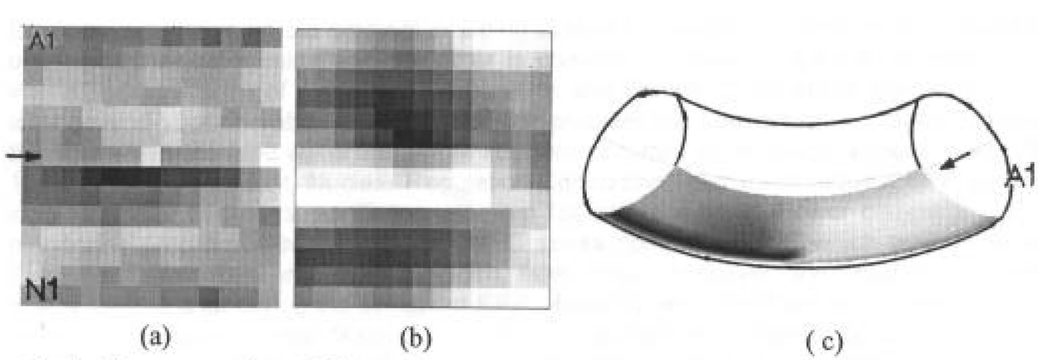

Fig 5. The comparison of inspection and prediction data for elbow 2037 (a) thickness (thick location marked in black) (b) wear rate (severe wear location marked in black) (c) prediction (obvious wear location marked in black)

RESULTS AND DISCUSSIONS

The original wall thickness, the managed wear rate and the calculated data for the three components of the HPTB extraction piping, that is N1P, E2036 and E2037, are shown in Figures 3 to 5, respectively. The severity of each case is represented by gray level. It is worth to note that the absolute value is not necessary but the relative one for the present purposes which is the prediction of the most probable wear locations. First of all, it is noted the averaging process to smear out peculiar trend of data do work and provide more clear physical explanations, as shown in the part (a) and part (b) of Figure 3 to Figure 5 . So the wear rate data will be used for the verifications of the analysis.

Figure 3(b) shows that the locations with higher wear rate almost distribute in the regions from M to B (clockwise azimuthal) and from 4 to 7 (axial), i.e. darker regions. However, the bursting location of N1P in #2 is six inches below the welding, that is the location between A2 and A3 in Figure 3(b). Although there are actually a little difference for the wear location between these two cases, it is reasonable to look the cases as the same. For any cases, it is obvious that the inlet or upstream conditions play an important role. Since there will be no any serious wear if the extraction flow comes in the piping uniformly, even the flow pattern is two-phase droplet flow. It is the geometry of the circumferential cavity, which is located just upstream of N1P and the steam is sucked in, plays the most dominant role and directs the flow directly onto the inner wall surface of the N1P. However, the precise wear locations may depend on inlet velocity, void fraction and droplet size besides the upstream geometry. Figure 3(c) shows the wear distributions of the same case by the present analysis. It is obvious that the present calculations could almost simulate the locations with higher wear rate, although the regions may be somewhat bigger or smaller. The droplet size is important in determining the axial location, for example. The heavier droplets may affected a longer regions of the wall in axial but the lighter one do shorter due to the competitions among the viscous, the inertia and the gravitational force. The present droplet diameter in the analysis is assumed to be 1mm. The distributions of the severity of wear rate for E2036 are shown in the Figure 4(b). The most dominant wear regions range from K to D and from 6 to 10, and are almost centered at A8, which are the downstream and outside part of the elbow. Obviously, the locations with higher wear rate are just the same as expected from experiences. The calculated results that show the same trends as inspection data and expected one are shown in the Figure 4(c). It is not surprising to expect such a result since the upstream piping of the elbow is straight and L/D is long enough to cause the flow uniform, especially for droplet not to impinge wall directly. Moreover, the flow with heavier droplets will cause more serious thinning rate on the more upstream region of the elbow due to the effects of inertia.

As for the other elbow, E2037 in the analysis, the locations with higher wear rate is not distributed along the center line of the outside wall (A1 to A13) as usually expected but both sides of that, and located somewhat downstream parts of the elbow. That is the regions ranged from C to F and from 3 to 8, and the regions ranged from K to M and from 1 to 6 in the Figure 5(b). The distributions of wear rate by inspections and calculations are shown in Figure 5 (b) and (c), respectively. The comparisons show that the predictions simulate the major trends but only one side of the wear. The reason why might be attributed to the only one droplet size selected in the calculations. Because the piping between E2036 and E2037 is short and horizontal, the gravitational effects may be significant for the flow with heavier droplets and the swirling effects due to two perpendicular elbow are also important . However, The behavior of the droplets might still be the consequences of the competitions among the inertia, the gravitational and viscous force. In the reality, the droplet size will not be single but wide range of sizes. The heavier droplets may have a lot of chances to flow along the lower part of the elbow while the lighter droplets upper part. That might be the reason why the wear regions separated into two parts.

CONCLUSIONS

An approaching method to predict the most probable regions with higher wear rates is developed and the break incident of HPTB extraction piping in the Maanshan NPP is also introduced for comparisons in the present paper. The conclusions are drawn as follows

1. The local locations of piping with higher wear rate could be predicted by the present CFD technique and wear model, However, the improvements of accuracy still need more efforts.
2. The relative upstream or downstream piping layout, the liquid volume fraction and the liquid droplet size are important factors in determining the locations with higher wear rates.
3. The break incident of HPTB extraction piping in the Maanshan NPP may teach us that other evaluation method may be necessary to help manage the monitoring program, i.e. to predict the most dangerous local regions of piping during management of the monitoring program.

REFERENCES

Chexal, V. K., R. Mahini, D. P. Munson, G. A. Randall, V. C. Shevde and J. S. Horowitz, “Recommendations for An Effective Flow-accelerated Corrosion Program”, NSAC-202L, 1993.

“CFDS-FLOW3D User Guide”, Computational Fluid Dynamics Service, 1994.

“Metals Handbook”, Ninth Edition, Vol. 13, ASM international, 1988.

Ma, Y. P., Y. M. Ferng and N. M. Chung, “ The Effects of Flow Field On Erosion/Corrosion and Its Application On Monitoring in Nuclear Power Plant”, Report, Taiwan Power Company, 1996.

Nesic, S and J. Postlethwaite., “A Predictive Model for Localized Erosion-Corrosion”, Corrosion, Vol.47, No. 58, p. 582, 1991.

Richard G. Keck and Peter Griffith, “Models and Equations for the Prediction of Erosive-Corrosive Wear in Steam Extraction Piping”, ASME, 87-JPGC-Pwr-35, 1987.

KEY WORDS

Erosion/Corrosion, Wear, piping, CFD, Two-Phase Flow, UT, Nuclear Power Plant.